

Spatial and temporal distribution of the adherens-junction-associated adhesion molecule A-CAM during avian embryogenesis

JEAN-LOUP DUBAND¹, TOVA VOLBERG², ILANA SABANAY², JEAN PAUL THIERY¹ and BENJAMIN GEIGER²

¹Laboratoire de Physiopathologie du Développement du Centre National de la Recherche Scientifique et de l'Ecole Normale Supérieure, 46 rue d'Ulm, 75230 Paris Cedex 05, France

²Department of Chemical Immunology, The Weizmann Institute of Science, 76100 Rehovot, Israel

Summary

A-CAM (adherens-junction-specific cell adhesion molecule) is a calcium-dependent adhesion molecule which is associated with intercellular adherens junctions in various tissues (Volk & Geiger, 1986, *J. Cell Biol.* 103, 1441–1450 and 1451–1464). In the present report, we have investigated the distribution of A-CAM during avian morphogenesis by immunofluorescence microscopy and immunoblotting. A-CAM appeared at the onset of gastrulation on developing mesodermal and endodermal cells and was then expressed on tissues derived from the three primary germ layers. During embryonic life, A-CAM was constitutively expressed in a number of tissues including the central and peripheral nervous system, myocardium, muscles, notochord, skin and lens whereas it was found transiently in many tissues ranging from the nephritic tubules and the endoderm of visceral arches to ectodermal placodes. In the adult, in addition to the nervous system, A-CAM was restricted to the skin, lens, heart and testis, and exhibited an apparent molecular weight higher than the one found in the embryo. The prevalence and cell-surface modulation of A-CAM could frequently be correlated with morphogenetic events such as mesenchyme condensation into epithelia or cell clusters (e.g. formation of the somitic epithelium, kidney tubules and peripheral ganglia), dissociation of epithelia (e.g. dissociation of the somitic epithelium and segregation of neural crest from the neural tube), separation of cell populations (e.g. fibroblasts and myotubes in the heart) and reorganizations of epithelia (e.g. neurulation). In addition, using electron microscopy, the expression of A-CAM on the surface of aggregating and separating cells could be correlated with the formation and disappearance of adherens junctions. This precisely scheduled control of A-CAM correlated with early morphogenetic events during embryogenesis suggests that this CAM could play a crucial role in these processes.

Key words: avian embryo; tissue remodelling; adherens junctions; cell adhesion molecules.

Introduction

Early morphogenesis proceeds in part by means of successive reorganizations of tissue sheets *via* processes such as cell migrations, mesenchyme condensations into epithelia, foldings and dissociations of epithelia and separations of diverse cell types. The occurrence of these diverse types of tissue remodelling has been correlated with the expression, prevalence and cell surface modulation of a group of molecules implicated in cell–cell adhesion and termed cell adhesion molecules (CAMs; for reviews,

see Edelman, 1985, 1986; Edelman & Thiery, 1985; Öbrink, 1986). Such is the case, for instance, of neurulation where both the neural CAM (N-CAM) and N-cadherin appear coincidently with the development of the neural epithelium whereas the liver CAM (L-CAM) becomes excluded from this tissue (Thiery *et al.* 1982, 1984; Edelman *et al.* 1983; Crossin *et al.* 1985; Hatta & Takeichi, 1986). Similarly, the formation of kidney tubules is accompanied by the appearance of N-CAM and N-cadherin which are subsequently replaced by L-CAM as the tubules mature (Thiery *et al.* 1982, 1984; Crossin *et al.* 1985; Hatta *et*

al. 1987). On the other hand, the sequence of events occurring during the development of feathers correlates with periodic and reiterative expressions of both N-CAM and L-CAM (Chuong & Edelman, 1985*a,b*; Crossin *et al.* 1985).

The study of distribution of the various known CAMs during embryogenesis has led to the distinction of two families: on one hand, the primary CAMs as defined by their very early appearance and their wide occurrence in tissue deriving from different germ layers; on the other hand, the secondary CAMs that appear secondarily on a limited number of differentiated tissues. So far, only primary CAMs were shown to distribute in correlation with processes of tissue remodelling. These include in all vertebrates N-CAM and more particularly its $140 \times 10^3 M_r$ form (Thiery *et al.* 1982; Edelman *et al.* 1983; Crossin *et al.* 1985; Murray *et al.* 1986), L-CAM (Hyafil *et al.* 1980; Damsky *et al.* 1983; Edelman *et al.* 1983; Thiery *et al.* 1984; Crossin *et al.* 1985), N-cadherin (Hatta & Takeichi, 1986; Hatta *et al.* 1987), in the rat species cell-CAM 105 (Ocklind *et al.* 1983; Odin & Öbrink, 1986) and in the mouse P-cadherin (Nose & Takeichi, 1986).

Another junctional CAM of $M_r 135 \times 10^3$ has been isolated from purified chick cardiac intercalated disks (Volk & Geiger, 1984). This molecule termed A-CAM (i.e. adherens-junction-specific cell adhesion molecule) is tightly associated with the plasma membrane of intercellular adherens-type junctions of a variety of cell types, such as chick cardiac myocytes and lens cells (Geiger *et al.* 1985*a*; Volk & Geiger, 1986*a*). A-CAM is apparently an integral membrane glycoprotein with an extracellular domain of at least 90×10^3 (Volk & Geiger, 1986*a*). In addition, the function of the A-CAM molecule appears to depend on calcium. Indeed, after chelation of extracellular calcium ions, adherens junctions between cultured epithelial lens cells are dissociated and the actin microfilament bundles are disorganized (Volk & Geiger, 1986*a*). Addition of calcium can restore these junctions along with the microfilaments network (Volk & Geiger, 1986*a*) and this reconstitution can be specifically inhibited by monovalent, but not divalent, antibodies to A-CAM (Volk & Geiger, 1986*b*). Recently, A-CAM has been shown to share significant functional homology with L-CAM: these two molecules being apparently involved in heterophilic interactions (Volk *et al.* 1987). Thus, A-CAM has been proposed to participate in intercellular adhesion in adherens junctions and to control indirectly the assembly of microfilament bundles (Volk & Geiger, 1986*b*). In many of its properties, A-CAM shows similarity to N-cadherin (Hatta & Takeichi, 1986) though the exact molecular interrelationships between them are not yet clear (see Discussion). The

subcellular distribution and the function of A-CAM are therefore indicative of a possible involvement of this molecule in the process of morphogenesis in the early embryo. In addition, since A-CAM is associated with adherens-type junctions, it constitutes an excellent marker for the formation of these junctions during embryogenesis.

In the present study, we have examined the tissue distribution of A-CAM in connection with the presence of adherens junctions during morphogenesis of the chick embryo by *in situ* immunofluorescence, electron microscopy and immunoblotting. Our results show that, in the embryo, A-CAM is widely distributed in many tissues derived from the three primary germ layers, whereas, in the adult, it is restricted to a limited number of tissues, including the heart and the lens. The localization and expression of A-CAM in adherens junctions are sharply regulated in connection with morphogenetic tissue remodelling. Finally, we show here that A-CAM is found in two forms differing in their molecular weight in adult and in embryonic tissues.

Materials and methods

Embryos

White Leghorn chick embryos were used throughout the study. Eggs were incubated at $37 \pm 1^\circ\text{C}$ in a humidified air chamber. Development of embryos at presomitic stage and with full number of somites was determined by reference to the staging series of Hamburger & Hamilton (1951). At other stages, ages were estimated by the number of somite pairs.

Antibodies

Mouse monoclonal antibodies to A-CAM (clone ID 7.2.3.) were produced as described previously (Volk & Geiger, 1984). Rabbit antibodies to L-CAM were kindly provided by G. M. Edelman (The Rockefeller University, New York).

Histological sections

Embryos were routinely fixed at room temperature in 3% formaldehyde in phosphate-buffered saline (PBS) for 1–4 h, depending on the size of the embryos. After extensive washes in PBS, embryos were embedded in a graduated series of sucrose solutions in PBS (12–25% wt/vol.) and frozen in Tissue Tek (Lab-Tek Products) in liquid nitrogen. Sections were cut at $5\text{--}8\ \mu\text{m}$ on a cryostat (either Bright Instrument Co. Ltd, Huntingdon, UK or Jung-Reichert Frigocut 2800, FRG) and mounted on slides coated with gelatin according to the procedure established by Lohmann *et al.* (1981).

Immunofluorescent staining

Immunofluorescent staining for A-CAM was performed essentially with the same procedure as described previously

for cell cultures (Geiger *et al.* 1985a). Briefly, sections were first dipped in a 50 mM-morpholinoethanesulphonic acid (MES) solution with 0.5 % triton X100, rinsed in PBS and incubated for 1 h with undiluted hybridoma supernatant. This was followed by an incubation with rhodamine lissamine B-sulphonyl chloride-conjugated rabbit monovalent antibodies to mouse immunoglobulins. Immunofluorescent staining for L-CAM was performed as described elsewhere (Thiery *et al.* 1984). Sections were observed with either a Zeiss or a Leitz epifluorescent microscopes.

Transmission electron microscopy

Embryos were fixed in 2 % glutaraldehyde, 3 % formaldehyde, 0.5 % acrolein, 5 mM-CaCl₂ in 0.1 M-cacodylate buffer pH 7.2 for 30 min, then rinsed and postfixed for 30 min with 1 % OsO₄ in cacodylate buffer. The blocks were dehydrated in ethanol and embedded in Polybed 812 (Polysciences, USA). Sections were stained with uranyl acetate and lead citrate and examined in a Philips EM410 electron microscope at 80 kV as described previously (Volk & Geiger, 1984).

Immunoblotting analysis

Samples of embryonic (5-day-old) and adult chick lens and heart tissues were trimmed, briefly homogenized and extracted at 100°C with SDS-sample buffer under reducing conditions. The extracts were clarified by centrifugation and subjected to SDS-PAGE followed by immunoblotting analysis with anti-A-CAM as described in Volk & Geiger (1986a).

Results

Appearance of A-CAM; distribution during gastrulation

A-CAM was first detected during gastrulation at stage 3 of Hamburger & Hamilton. It was present on cells that have ingressed from the developing primitive streak but not on epiblast cells (Fig. 1A-C). At the full primitive streak stage, i.e. stage 4 of Hamburger & Hamilton, ingression of cells from the primitive streak has reached its maximum, mesodermal cells actively migrate under the epiblast and the definitive endoderm is laid down (for details, see Vakaet, 1970). Staining for A-CAM was found on cells that have detached from the primitive streak, on migrating mesodermal cells and on endodermal cells (Fig. 1D-F). Interestingly, the staining was preferentially accumulated in areas of cell-cell contact (Fig. 1F). From stage 5 of Hamburger & Hamilton onwards, the primitive streak regresses in size leaving the notochord rostral to Hensen's node (for details, see Vakaet, 1970). Staining for A-CAM was essentially similar to that at stage 4, except that the notochord was markedly labelled and that cells located in the groove of the primitive streak were also stained (Fig. 1G-I). In contrast, epiblastic cells

located lateral to the groove of the primitive streak and rostral to the Hensen's node remained negative for A-CAM (Fig. 1G,H).

Neurulation

The neural plate appears soon after the regression of the primitive streak. In the head and rostral part of the trunk, it forms by local thickening of the epiblast ahead of Hensen's node along the axis of symmetry of the embryo. No A-CAM-specific fluorescence staining could be detected in the neural plate at this stage (Fig. 1H). The neural plate subsequently undergoes a process of folding both medially and laterally resulting in the appearance of a V-shaped structure. The apparent expression of A-CAM on the neural plate started at the initiation of this process. Distribution of A-CAM was restricted to the medial portion of the neural plate (Fig. 2A). Moreover, this distribution was polarized such that only the subapical region of the neural epithelium was stained (Fig. 2).

The distribution of A-CAM changed gradually with the closure of the neural tube. As the neural epithelium formed a deep groove, staining for A-CAM on the apical side of the neural epithelium expanded progressively nearly up to the neural folds at the boundary with the ectoderm (Fig. 2C; see also Fig. 4A,B). In addition, A-CAM could also be detected in the lateral surfaces of the neural epithelial cells while it was still present in high amounts in their apical side (Fig. 2D). The extensive distribution of A-CAM in the neural tube could be correlated with the presence of a conspicuous zonula adherens along the subapical borders of the cells (Fig. 3A,B).

After the closure of the neural epithelium into the neural tube, A-CAM was distributed throughout the tissue, but the intensity of the staining varied locally (Fig. 2E). In particular, the lateral sides of the neural tube were heavily stained whereas dorsally, in the area facing the ectoderm, the staining was weaker (Fig. 2E). At the cellular level, A-CAM was found on the lateral surfaces of the neural cells, in addition to the previously described subapical surfaces where it was predominantly accumulated (Fig. 2F).

Later on, prior to neuronal differentiation, A-CAM staining increased in intensity so that it was found in nearly equal amounts on both the subapical and basolateral surfaces of the neural epithelium cells (see Fig. 4C). Upon neuronal differentiation and appearance of multiple layers in the neural tube, the distribution pattern of A-CAM changed considerably and became complex. For example, in the trunk, fibres stretching from the outer to the inner surfaces of the spinal cord were characterized by their strong expression of A-CAM whereas motoneurons were more weakly labelled (not shown).

It should be noted that the process of neural tube

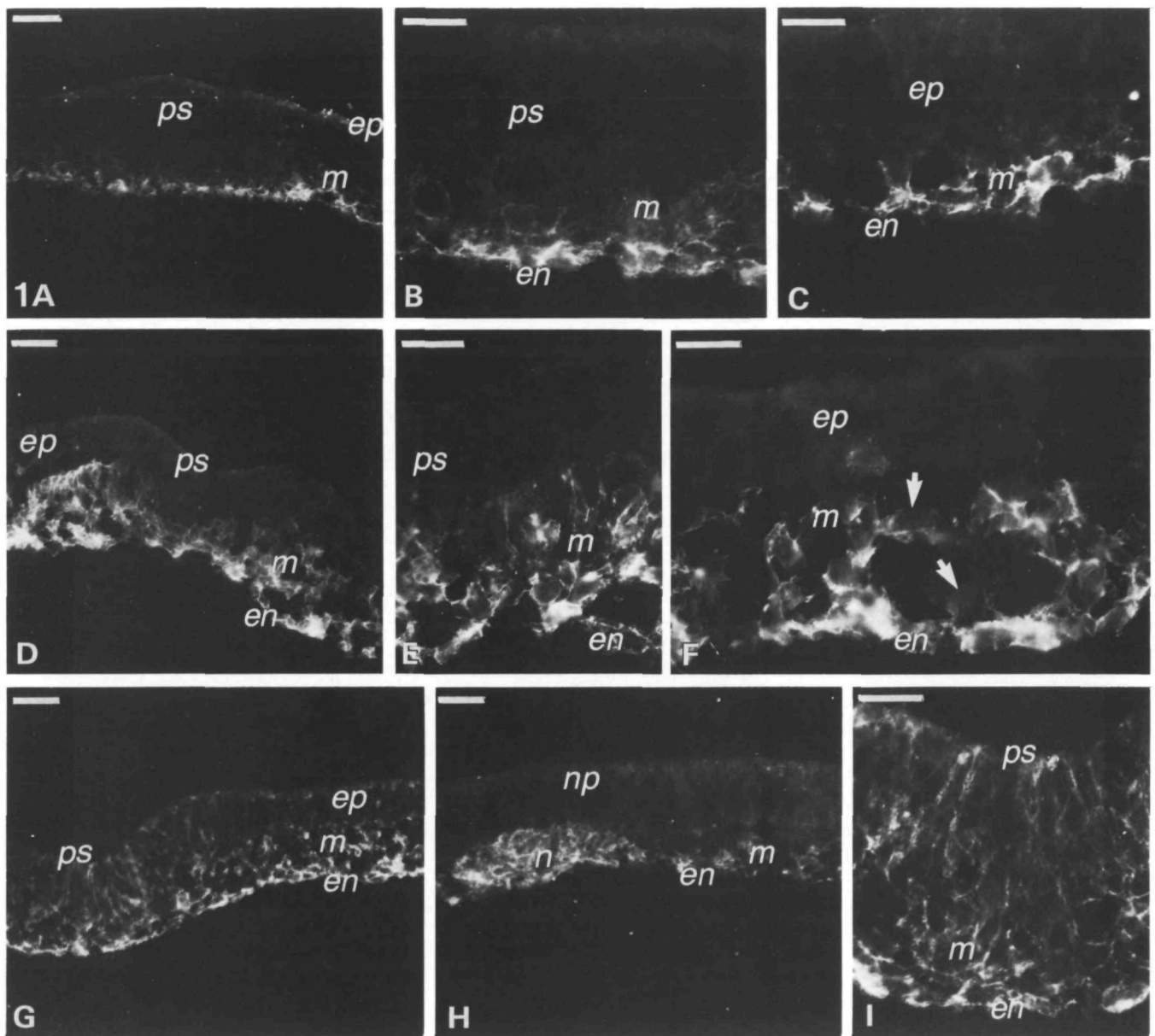


Fig. 1. Distribution of A-CAM during gastrulation. Transverse sections through the blastoderm at the short (A–C), full (D–F), and regressing (G–I) primitive streak stages respectively corresponding to stages 3, 4, and 5 of Hamburger & Hamilton. (A,D,G) represent overviews of the blastoderm in the primitive streak region and (B,E,I) and (C,F) show details of cells respectively in and lateral to the primitive streak. (H) Corresponds to area of the developing notochord rostral to the regressing primitive streak. At stages 3 and 4, A-CAM staining is restricted to endodermal cells and to mesodermal cells that have fully detached from the epiblast and are migrating under the epiblast. Note that labelling is found almost exclusively in the areas of cell–cell contact between mesodermal cells (arrows in F point to the unstained cell membranes that are not in contact with other cells); in addition, cells of the endoblast are only stained on their surfaces facing mesodermal cells. At stage 5, A-CAM staining is still visible on endodermal and mesodermal cells and more particularly on the notochord; in addition, it is also present on the epiblast in the primitive streak but not on the thickening neural plate. *en*, endoderm; *ep*, epiblast; *m*, mesoderm; *n*, notochord; *ps*, primitive streak. (A,D,G,H) bar, 50 μ m; (B,C,E,F,I) bar, 25 μ m.

formation is not the same along the whole embryonic axis. In particular, in the caudal part of the trunk, the neural tube does not form by folding of the neural epithelium but by regrouping of cells and formation of a cavity among them. The distribution of A-CAM

was seen to vary accordingly. Prior to their regrouping, presumptive neural epithelium cells exhibited a mesenchymal organization and were weakly stained for A-CAM. This staining increased in intensity as cells became closely associated with their neighbours.

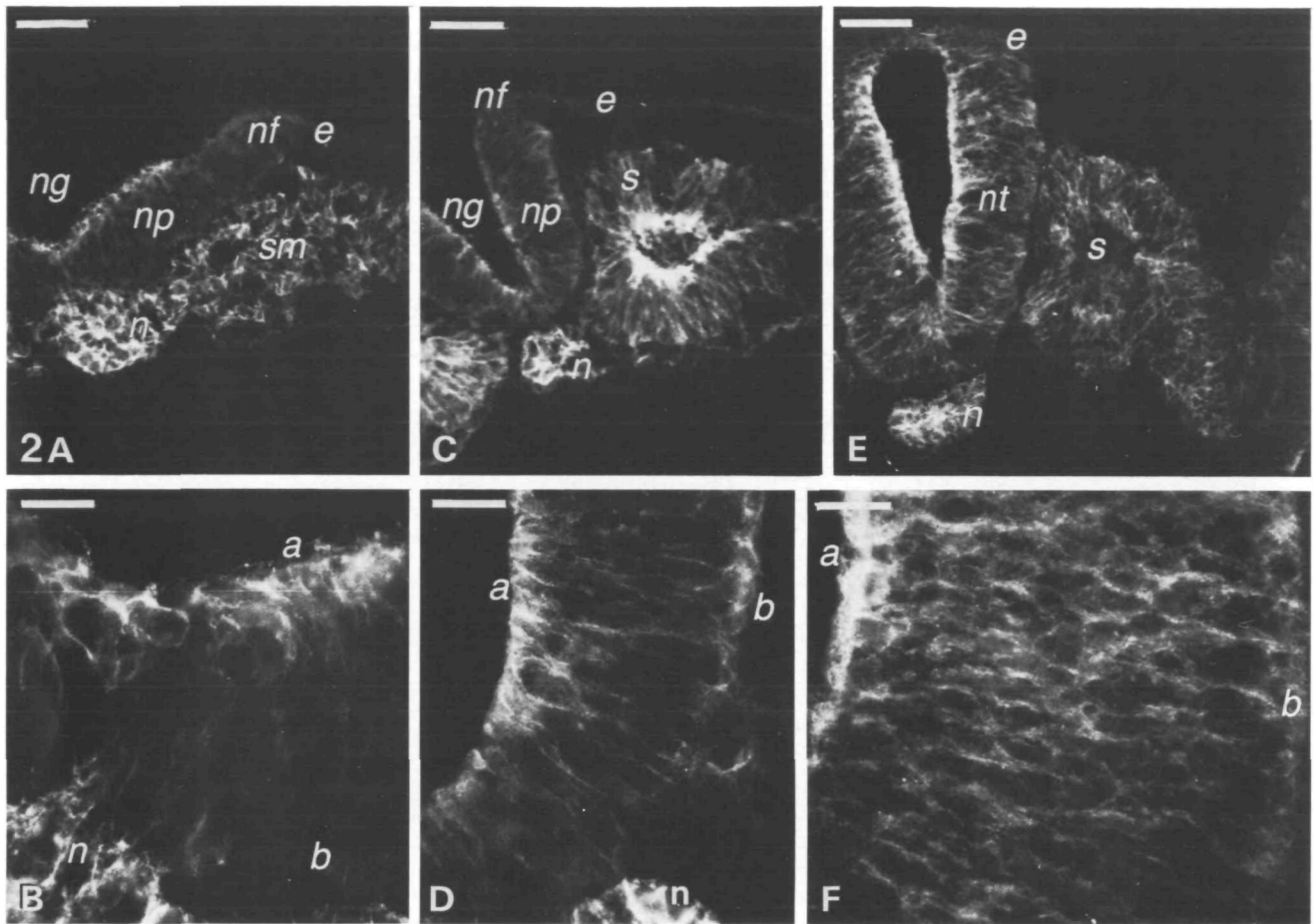


Fig. 2. Distribution of A-CAM during neurulation in the trunk. Three characteristic stages of neurulation in the trunk region are shown: these are the invaginating neural-plate stage (A,B), the neural-fold stage (C,D), and the neural-tube stage (E,F). (A,C,E) show the distribution of A-CAM at the tissue level and (B,D,F) at the cellular level. As the neural tube is developing and closing, A-CAM expression expands progressively from the subapical surfaces of cells located in the ventral side of the neural epithelium first to both the subapical and basal surfaces of cells present in the ventral and lateral sides of the neural epithelium and finally to the whole surface of all the cells. *a* and *b* indicate the apical and basal surfaces of neural epithelial cells; *e*, ectoderm; *n*, notochord; *nf*, neural fold; *ng*, neural groove; *np*, neural plate; *nt*, neural tube; *s*, somite; *sm*, somitic mesoderm. (A,C,E) bar, 50 μ m; (B,D,F) 25 μ m.

With the appearance of cavities among cell clusters, A-CAM was polarized in the areas facing the cavities. Later on, when the various cavities have fused into a typical lumen, A-CAM followed the same distribution pattern as that described for more anterior levels (data not shown).

Segregation and early migration of neural crest cells from the neural tube

Prior to their emigration, the presumptive neural crest population is integrated in the neural folds at the boundary between the ectoderm and the neural epithelium. In the avian embryo and more particularly at cephalic levels, the segregation of the neural crest from the neural tube is directly connected with the fusion of the neural folds and the closure of the

neural tube (for a review, see Duband & Thiery, 1985).

In the head, premigratory neural crest cells expressed A-CAM, but the staining was less prominent than on the neural epithelium (Fig. 4A,B). At the apposition of the neural folds, whereas A-CAM staining increased on cells in the neural epithelium, it became apparently undetectable on premigratory neural crest cells (Fig. 4C). By electron microscopy, no adherens-type junction could be visualized among this population (Fig. 5A,B). As neural crest cells underwent their active migration away from the neural tube, they remained devoid of A-CAM (Fig. 4D,E). During that time, the closure of the neural tube was on the way to completion: A-CAM staining was expanding more and more medially and the separation between neural crest and neural epi-

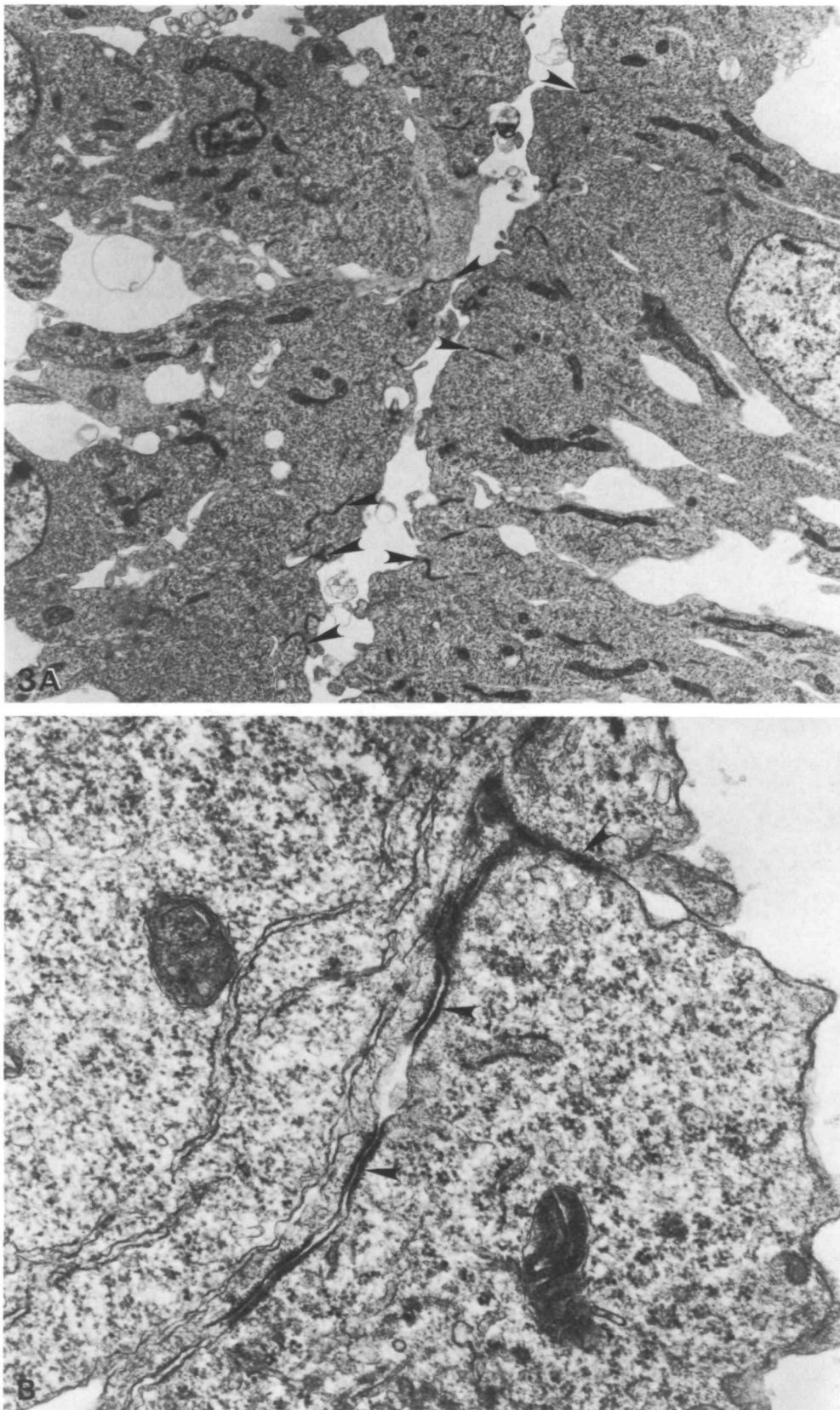


Fig. 3. Transmission electron micrographs of the truncal neural tube of a 3-day-old embryo. Both low-power (A) and high-power (B) magnifications of neural tube cells reveal numerous adherens-type indicated by arrowheads at the subapical region near the lumen. (A) $\times 3400$; (B) $\times 24000$.

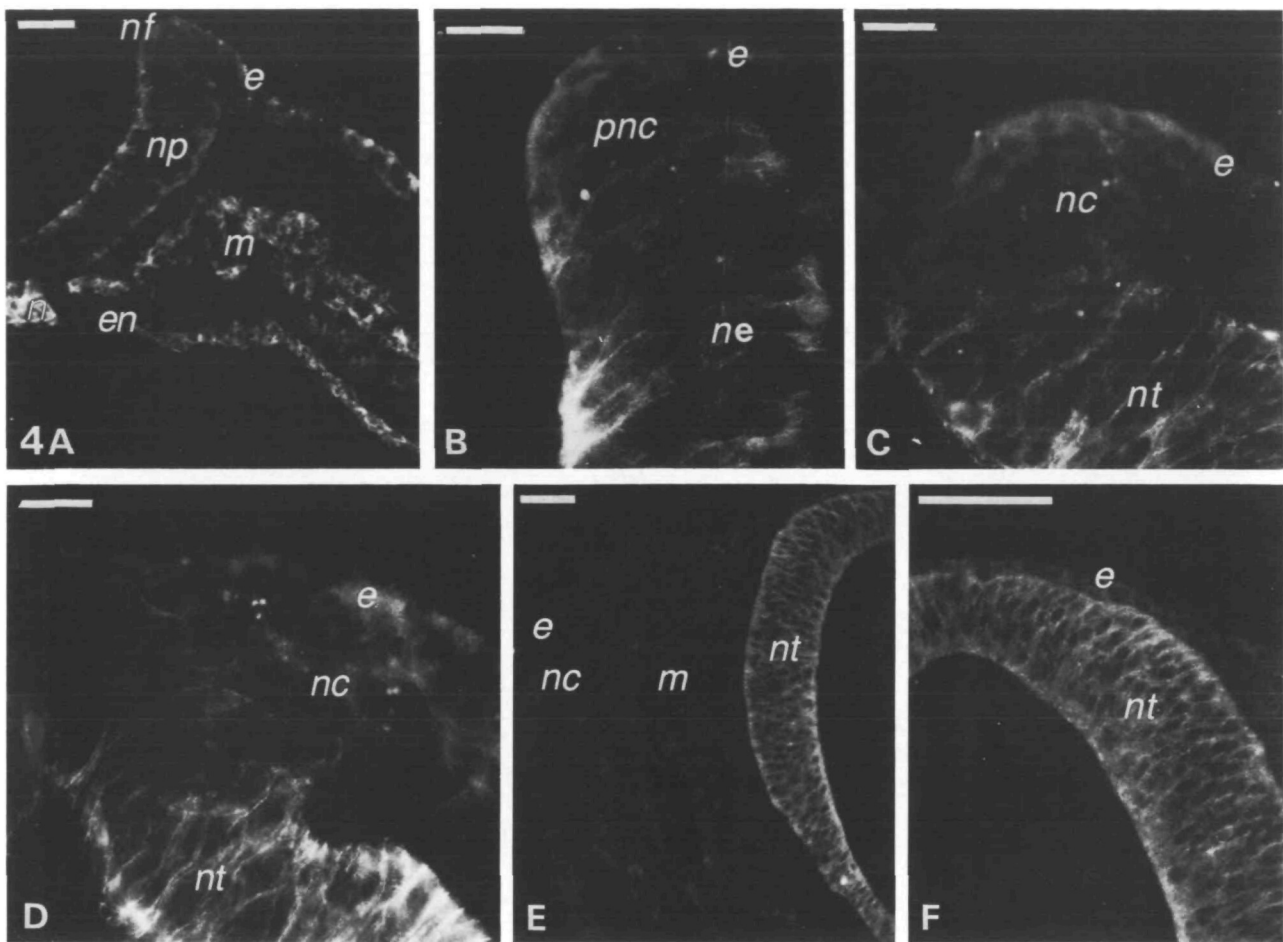


Fig. 4. Distribution of A-CAM during segregation and early migration of mesencephalic neural crest cells. (A,B) 4-somite stage showing the mesencephalon prior to neural fold fusion; (B) represents a detail of the presumptive neural crest population. Neural epithelial cells show A-CAM staining mostly on their subapical and basal surfaces whereas premigratory neural crest cells located in the folds are only weakly stained. (C) 6-somite-stage embryo. The folds are apposed and neural crest cells are about to emigrate; the latter are not or only weakly stained for A-CAM in contrast to the neural epithelial cells which show an increasing staining on their whole surface. The difference in the staining of the two populations allows the precise localization of the boundary between them. The apparent staining on the ectoderm and some of the neural crest cells corresponds to autofluorescence frequently observed in this area. (D) 8-somite stage. Neural crest cells have undergone their migration and the closure of the neural tube is complete. A-CAM staining is expanding to the medial part of the neural tube corresponding to its progressive closure. (E,F) 12-somite stage embryo showing in (E) migrating neural crest cells that are devoid of staining and in (F) a detail of the dorsal border of the neural tube after the last neural crest has emigrated. *e*, ectoderm; *en*, endoderm; *m*, mesenchyme; *nc*, neural crest; *ne*, neural epithelium; *nf*, neural fold; *np*, neural plate; *nt*, neural tube; *pnc*, premigratory neural crest. (A,E,F) Bar, 50 μ m; (B,C,D) 10 μ m.

thelial cells was underlined by the difference in A-CAM staining (Fig. 4C,D). After the complete closure of the neural tube and the complete emigration of neural crest cells, the dorsal aspect of the neural tube was entirely stained for A-CAM (Fig. 4F).

In the trunk of avian embryos, segregation of neural crest was more progressive than in the head and it was delayed with respect to neural tube closure. As shown previously (Fig. 2E), A-CAM staining was present throughout the neural epithelium but the intensity of the staining was slightly

lower on the dorsal aspect of the neural tube (i.e. the presumptive neural crest region) than on the lateral sides. In contrast to the cephalic levels, premigratory neural crest cells that were integrated into the neural epithelium were positively stained for A-CAM (Fig. 6A,B). Only neural crest cells that had fully separated from the neural tube and actively migrated were devoid of A-CAM (Fig. 6A–C).

Aggregation of neural crest cells into peripheral ganglia

At the end of its migration, part of the neural crest

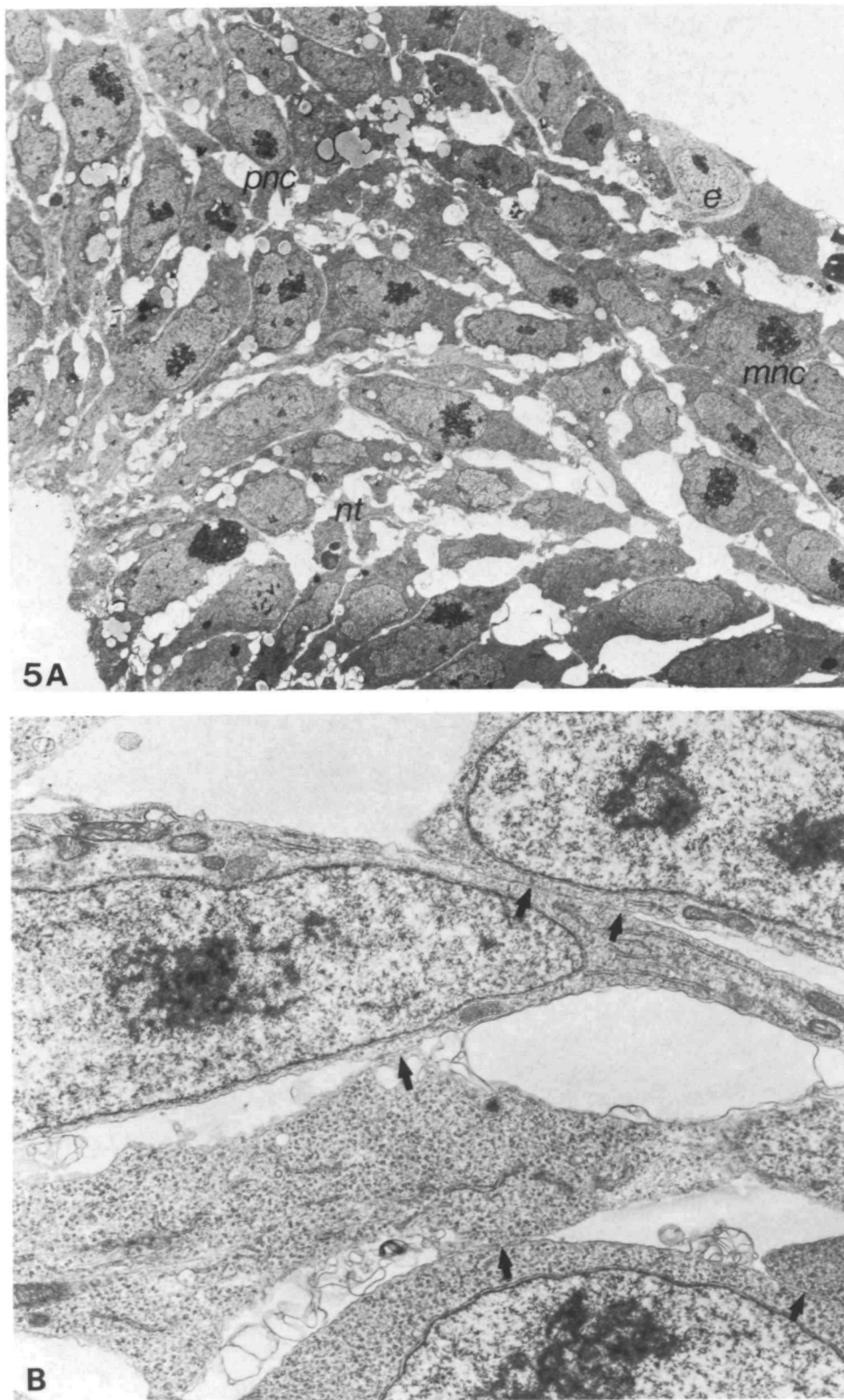


Fig. 5. Electron micrographs at low (A) and high (B) magnification showing premigratory neural crest cells in the mesencephalic region. Even though premigratory crest cells show large portions of their plasma membrane in contact with their neighbours, they lack adherens junctions. Arrows point at regions of the cells which are intimately associated with neighbouring cells. *e.* ectoderm; *mnc.* migratory neural crest cells; *nt.* neural tube; *pnc.* premigratory neural crest cells. (A) $\times 1150$; (B) $\times 11\,500$.

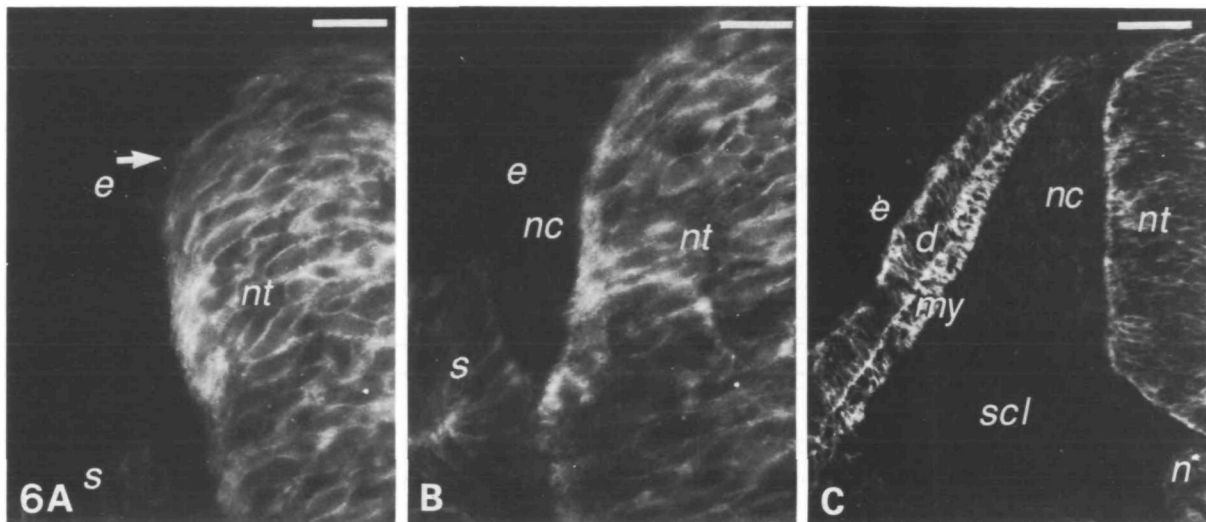


Fig. 6. Distribution of A-CAM during segregation and early migration of trunk neural crest cells. A, B and C show the 25th, 20th, and 10th somite levels of a 28-somite-stage embryo which are typical levels of the different steps of neural crest cell emigration. In A, neural crest cells are starting to leave the neural tube; only cells that are fully detached from the neural tube have lost their staining (arrow) whereas premigratory cells are still clearly stained. In B, the crest cell emigration process has amplified and migrating neural crest cells have reached the somitic area; premigratory crest cells are still positive for A-CAM. In C, the neural crest population has completely separated from the neural tube and is migrating along the neural tube and myotome; this population is characterized by its absence of A-CAM staining. *e*, ectoderm; *d*, dermatome; *my*, myotome; *n*, notochord; *nc*, neural crest; *nt*, neural tube; *s*, somite; *scl*, sclerotome. (A,B) bar, 10 μ m; (C) bar, 50 μ m.

population aggregates into compact structures that subsequently differentiate into ganglia of the peripheral nervous system. Such is the case, for example, of the spinal ganglia that form along the neural tube. As soon as neural crest cells started to accumulate and to form the primordium of the spinal ganglion, A-CAM staining which was not represented on the surface of migrating cells (see Fig. 6C) reappeared on the whole surface of aggregating cells (Fig. 7A). A-CAM was thereafter retained on spinal ganglion cells when neuronal differentiation occurred (Fig. 7B,C). It was detectable on both neuronal cell bodies and neurites and was also apparently expressed by non-neuronal cells (Fig. 7B,C).

A-CAM was also detected early during the process of formation of the sympathetic ganglia. It was found at high levels on sympathetic precursors even before their complete aggregation into clusters (Fig. 7D) and remained afterwards on the ganglion cells during the embryonic life (Fig. 7E,F). An intense staining for A-CAM could also be observed on various neural crest-derived peripheral ganglia such as the enteric (Fig. 7G), trigeminal (Fig. 7H), and ciliary (Fig. 7I) ganglia.

Formation and subsequent reorganization of somites

Somites are ball-shaped metameric units found along the body axis and constitute the primordia of the skull, muscles and dermis in the trunk. They pro-

gressively form from an apparently homogeneous rod of mesenchyme, the segmental plate, located in the caudal end of the embryo. The process of the formation of somites is continuous until the total number of segments is reached. Prior to their association into the somitic epithelium, mesenchymal cells of the segmental plate expressed A-CAM, the molecule being distributed throughout their surfaces (Fig. 8A). Interestingly, as seen by electron microscopy, adherens junctions were rarely seen on these cells (Fig. 9A,B). As segmental plate cells were progressively condensing into epithelial structures, A-CAM levels notably increased and the protein was apparently redistributed on their surfaces (Fig. 8B,C). It was predominantly located close to the apical side of epithelial cells, while it remained, though at apparently lower levels, on the whole surface of the non-epithelial cells of the core (Fig. 8C). The local concentration of A-CAM in the junction-rich areas was further evidenced by electron microscopy showing an abundance of these junctions in the subapical aspect of the somitic epithelium (Fig. 9C).

A few hours following their formation, somites undergo structural reorganizations which lead to their partition into, medioventrally, a mesenchyme termed sclerotome and, laterodorsally, an epithelium called dermamyotome. Such a reorganization was slightly preceded by the complete disappearance of A-CAM and adherens junctions from cells destined to form

the sclerotome while the staining was unchanged on the epithelial cells of the dermamyotome (Figs 8D,9D).

After the complete reorganization of the ventral

side of the somite into sclerotome, the single-layered epithelium of the dermamyotome undergoes transformations which lead to the formation of a double-layered epithelium, the dermatome and the myo-

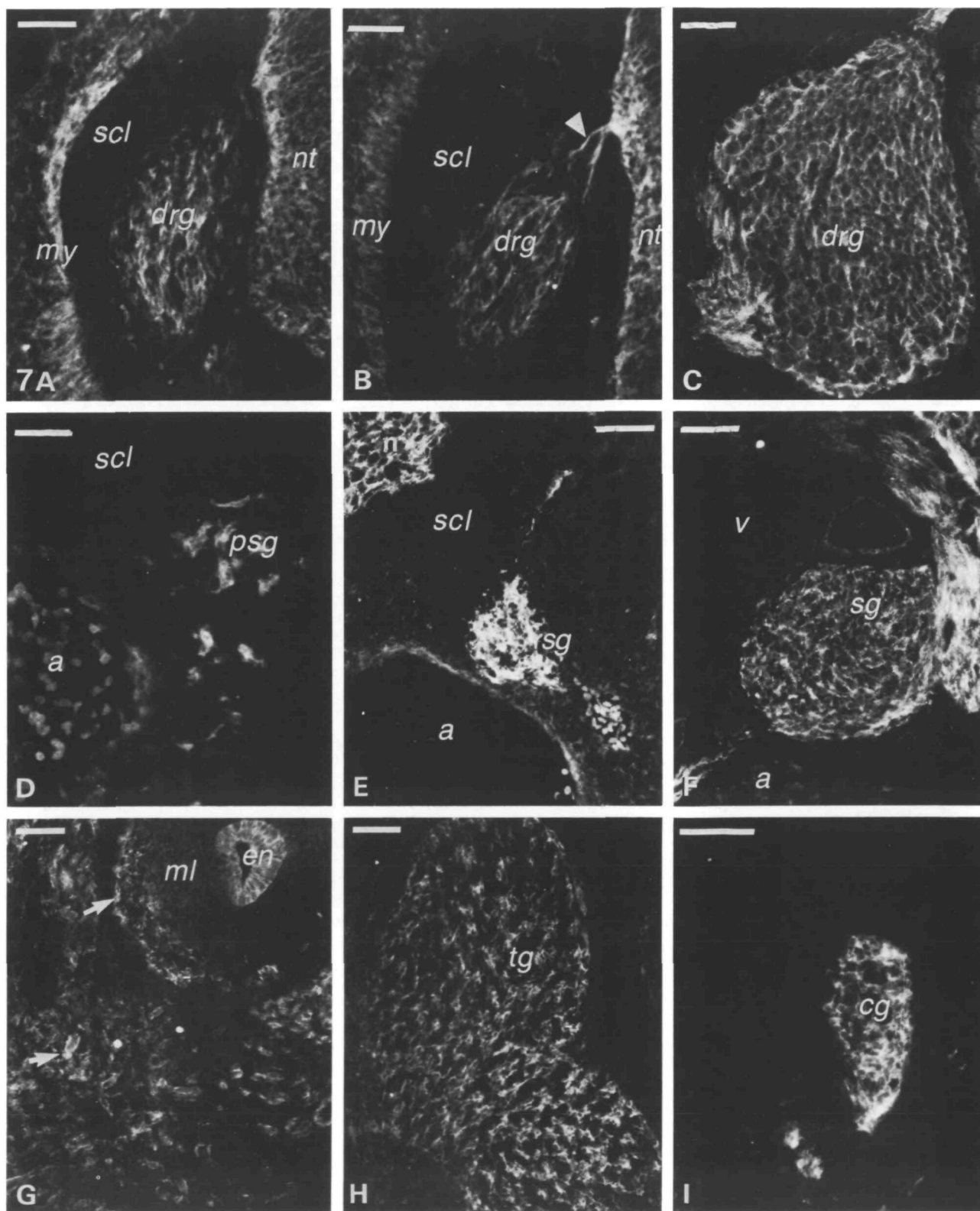


Fig. 7. For legend see p. 336

tome. The myotome develops from the extremities of the dermatomyotome. Cells that constituted the myotome were strongly stained for A-CAM as soon as they appeared (Fig. 8E,F); this staining remaining intense during the whole development of the myo-

tome and during myoblast differentiation (Fig. 8G-I). In addition, in contrast to dermatome cells that exhibited A-CAM mostly on their subapical surfaces, myotomal cells were stained on their entire surfaces (Fig. 8F,H). After the formation of the

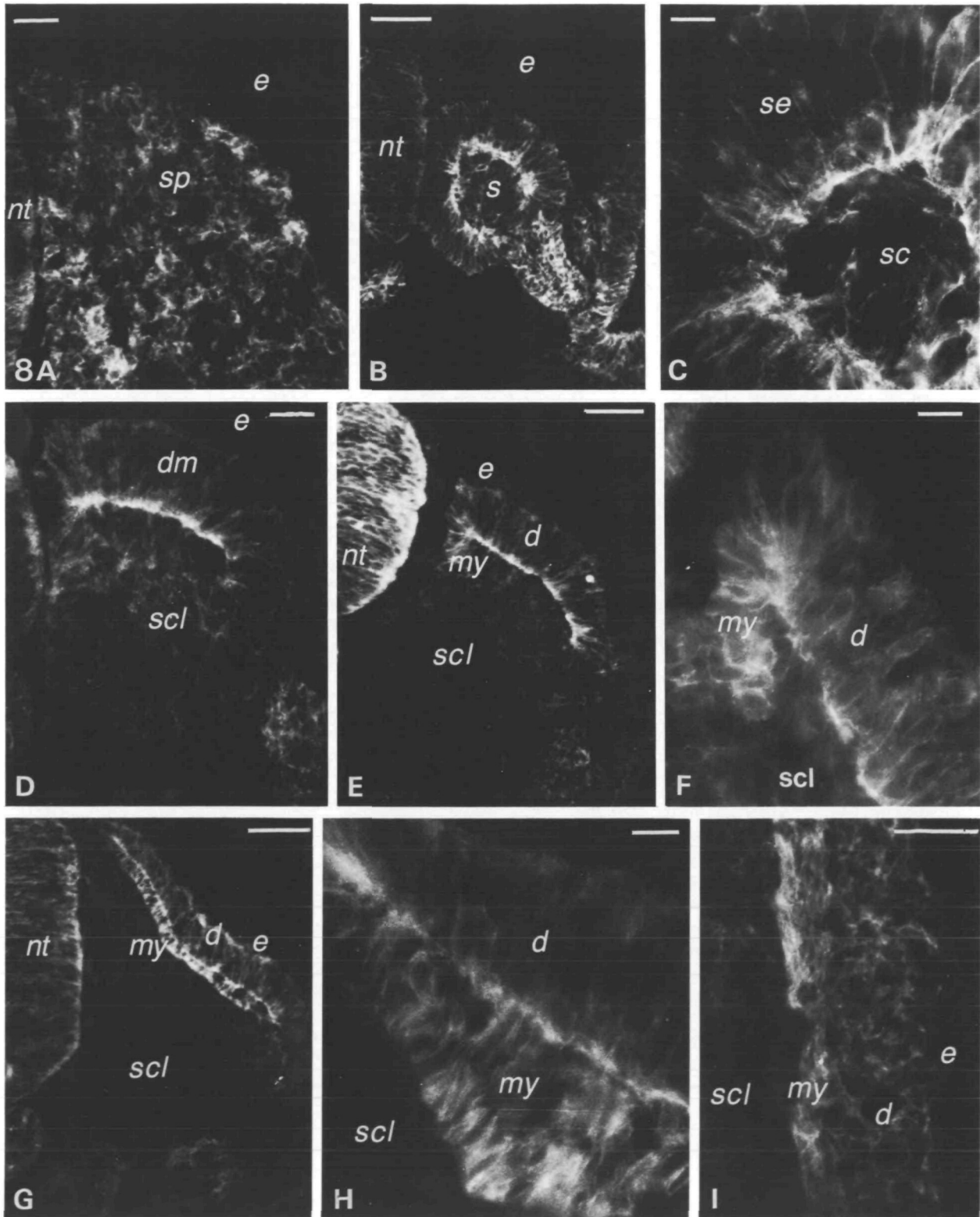


Fig. 8. For legend see p. 336

myotome and during myoblast differentiation into myotubes, the dermatome dissociates into the dermis of a mesenchymal organization. During this process, A-CAM was both redistributed and reduced in amount on the surface of the dermal cells (Fig. 8I).

Fig. 7. Distribution of A-CAM in developing peripheral ganglia. (A–C) Spinal or dorsal root ganglia at three stages of development, i.e. early aggregation at stage 21 of Hamburger & Hamilton (A), neurite outgrowth at stage 23 of Hamburger & Hamilton (B), and late differentiation at day 9 of incubation (C). A-CAM is detectable on presumptive spinal cells as soon as they aggregate into ganglia and remains present on all the cells during differentiation (arrowhead points at neurite fibres growing towards the neural tube). (D–F) Sympathetic ganglia at stages 21 and 23 of Hamburger & Hamilton and at day 9 of incubation. Presumptive sympathetic cells exhibit a strong staining for A-CAM just before they form a compact aggregate. Staining subsequently remains on cells during and after cellular differentiation. Note that nerves emerging from both spinal and sympathetic ganglia are also heavily stained for A-CAM. (G–I) Enteric, trigeminal and ciliary ganglia all show high levels of A-CAM as soon as they form. Note that enteric ganglia form in the A-CAM-rich environment of the muscular layer (short arrows point at ganglion cells). *a*, aorta; *cg*, cilia ganglion; *drg*, dorsal root ganglion; *en*, endoderm; *ml*, muscle layer; *my*, myotome; *n*, notochord; *nt*, neural tube; *psg*, presumptive sympathetic ganglion; *scl*, sclerotome; *sg*, sympathetic ganglion; *tg*, trigeminal ganglion; *v*, vertebra. Bar, 50 µm).

Fig. 8. Distribution of A-CAM during the formation and reorganization of somites. (A) Condensing segmental plate showing A-CAM on regrouping cells. (B,C) Fully condensed somite; A-CAM is expressed at high levels by epithelial cells where it is preferentially accumulated on their subapical surface whereas core cells are much less stained (C shows detail of the somite). (D) Beginning of the dissociation of the ventral side of the somitic epithelium. A-CAM is no longer expressed by the dissociating ventral cells destined to form the sclerotome in contrast to the more dorsal cells, the dermamyotome, that remain epithelial and show high levels of A-CAM. (E,F) Formation of the myotome. Myotomal cells growing from both the medial and the lateral side of the dermamyotome show a strong uniform staining for A-CAM (F shows a detail of the dermatome and of the developing myotome). (G,G) Fully developed myotome. A-CAM staining is still intense and diffuse on myotomal cells. (I) Development of the dermis. The dermatome dissociates into the mesenchymal dermis; A-CAM can be still detected on the dermis but it is uniformly distributed on the cell surfaces. Note the strong staining on elongating myotubes. *d*, dermatome; *dm*, dermamyotome; *e*, ectoderm; *my*, myotome; *nt*, neural tube; *s*, somite; *sc*, somite core; *se*, somite epithelium; *scl*, sclerotome; *sp*, segmental plate. (A,D) bar, 25 µm; (B,E,G,I) bar, 50 µm; (C,F,H) bar, 10 µm.

Morphological and histological formation of the heart

The heart derives in a large part from cells located in the lateral mesoderm at cephalic levels. This lateral mesoderm was found to express high levels of A-CAM very early after its appearance during gastrulation. The intensity of the staining on cardiac lateral mesoderm was noticeably higher than on the lateral mesoderm of other areas of the embryo (data not shown). After its appearance, the lateral mesoderm is positioned in medial areas by consecutive foldings leading to the formation of two and then one tubule. During this whole process, A-CAM remained at high levels on presumptive myocardial cells and was predominantly associated with the cell surfaces involved in cell–cell contact (Fig. 10A–C). In contrast to myocardial cells, endocardial and epicardial cells were totally devoid of A-CAM (Fig. 10C,E). A-CAM remained on myocardial cells at the time of formation of a multilayered myocardium and myotube differentiation (Fig. 10D). Further development of the heart occurred with the appearance of fibroblastic cells in the cardiac jelly beside muscular cells; while the latter cell still expressed high amounts of A-CAM, the former cells showed only a faint labelling (Fig. 10E).

Formation of nephritic tubules

The mesonephron arises from part of the lateral mesoderm termed intermediate mesoderm or nephritic blastema and lying between the somite and the splanchnic mesoderm. The intermediate mesoderm first assembled as a compact mesenchyme organizes as tubules under the inductive action of the Wolffian duct. The Wolffian duct is a solid cord that forms in the rostral part of the trunk and grows caudally along the lateral sides of the somites. It expressed A-CAM at the initial stages of its development and, upon maturation, lost it except in its growing tip (data not shown). Prior to induction by the Wolffian duct, the nephritic blastema was stained for A-CAM: this staining increased in amount when condensation of nephritic blastema occurred (Fig. 11A). A-CAM continued to be expressed on the development tubules where it was predominantly located on lateral surfaces (Fig. 11B). The expression of A-CAM on tubules was transient; A-CAM was lost first on primary tubules proximal to the Wolffian duct then, later on, on secondary tubules (Fig. 11C). In addition, the disappearance of A-CAM from tubules occurred progressively along a proximodistal gradient and coincidentally with the appearance of L-CAM in areas where A-CAM was no longer found (see Thiery *et al.* 1984). The same sequence of A-CAM expression was observed for the induction of the pronephric and metanephric tubules (data not shown).

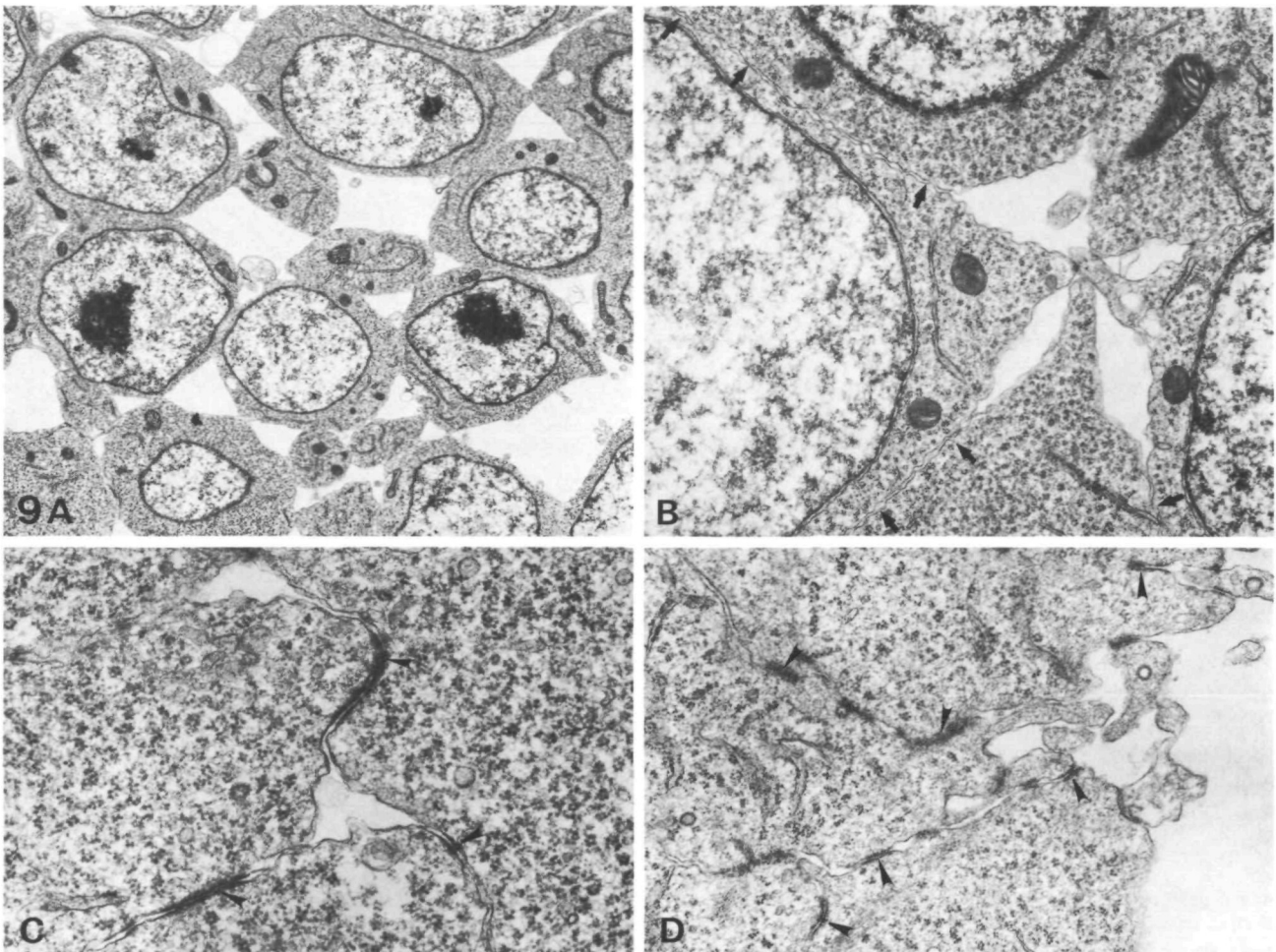


Fig. 9. Electron micrographs of the compacting segmental plate (A,B), the somitic epithelium (C) and dermatome (D). In contrast to segmental plate cells which show large areas of their surface in contact with their neighbours (arrows in B) but no adherens junctions, somite cells and dermatome cells that are integrated into epithelia possess numerous adherens junctions (arrowheads in C and D). (A) $\times 2870$; (B) $\times 7670$; (C) $\times 16\,000$; (D) $\times 16\,000$.

Ectodermal placodes, branchial arches, and other tissues

A-CAM was not usually found at high levels on ectodermal tissues. However, it was expressed on specialized regions of the ectoderm, particularly on placodes. For example, both the olfactory and lens placodes were precociously stained for A-CAM as soon as the thickening of the ectoderm could be visualized (Fig. 12A,B). Both olfactory and lens placodes retained A-CAM on their surfaces during their invagination and subsequent vesiculation (Fig. 12A,B), whereas the ectoderm that was overlying the vesicles was not stained (Fig. 12B). The pharyngeal placodes from which neurones of sensory ganglia of the head and neck derive were also seen to express significant amounts of A-CAM from the time of their appearance onwards (data not shown). In contrast to the other ectodermal placodes, the otic placode showed only low levels of labelling before it had deeply invaginated and acquired a tear-drop

shape. Later, A-CAM was expressed throughout the otocyst, yet at the initiation of the cochlear duct it appeared predominantly in the sensory part of the inner ear (Fig. 12C). Detailed characterization of A-CAM expression in the developing inner ear will be described elsewhere (Raphael, Y., Volk, T., Crossin, K., Edelman, G. M. and Geiger, B., in preparation). Finally, A-CAM was found transiently on the ectoderm in the primordia of feathers at the time of their budding (not shown).

A-CAM usually showed a transient and complex expression pattern on endodermal tissues. For example, it was found on the gut (see, in particular, Fig. 7G) and on the liver rudiment (not shown). Of particular interest were the branchial arches and clefts. In these areas, only the regions connecting the ectoderm and endoderm were particularly intensely stained, whereas more internal portions of the endoderm of the pharynx and lateral ectoderm were faintly labelled (Fig. 12D). In addition, the endoderm

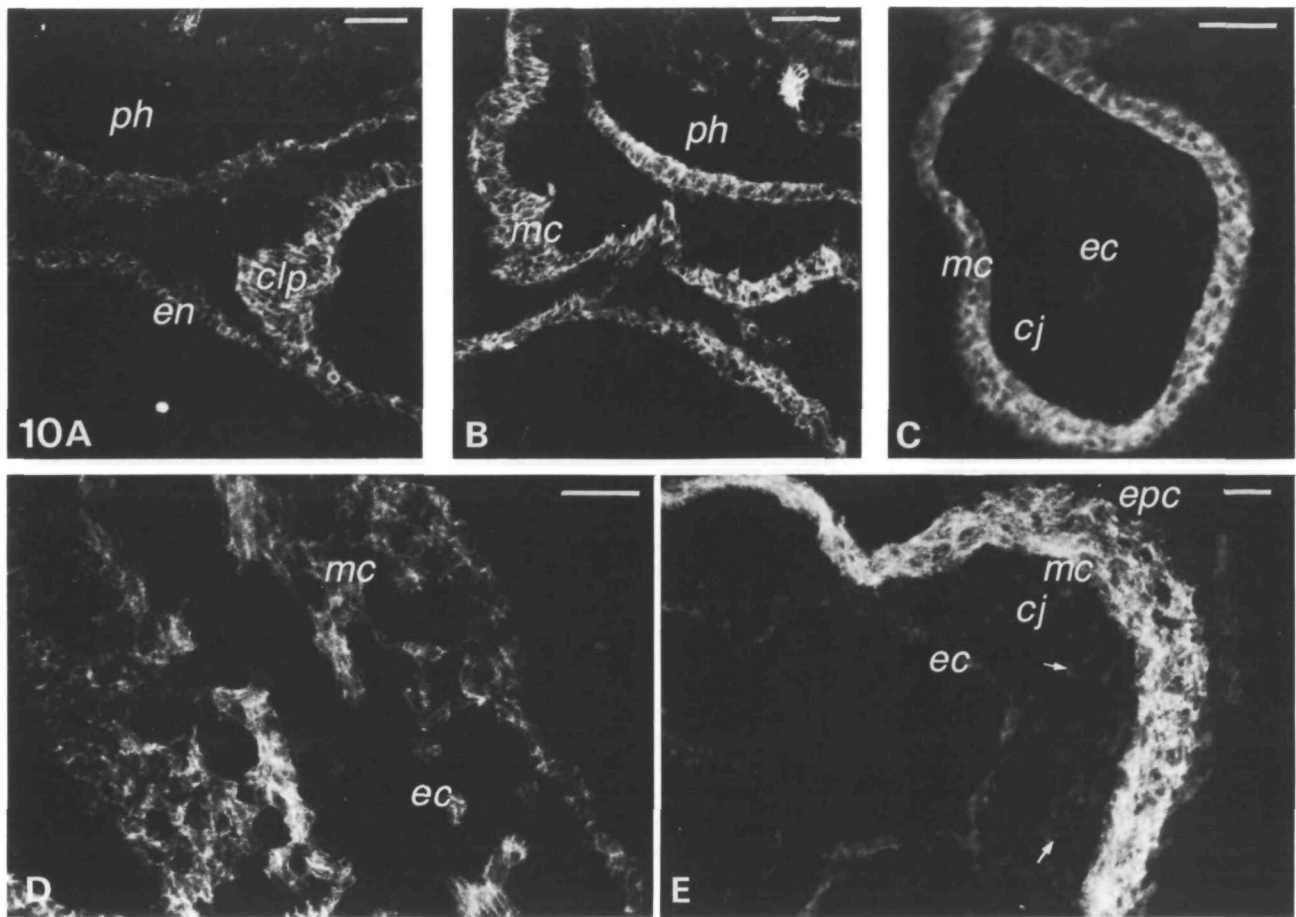


Fig. 10. Distribution of A-CAM during the morphogenesis and histogenesis of the heart. (A–C) Formation of heart tubule from the lateral plate at 8- to 12-somite stages. The epithelial-shaped lateral plate expresses high levels of A-CAM prior to and during its folding towards the midline of the embryo. Once the cardiac tubule is formed, endocardial cells move into it through the cardiac jelly. These cells are negative for A-CAM in contrast to the epimyocardium that is heavily labelled. (D) Formation of multiple layers in the epimyocardium. Both elongated and fibroblast-shaped cells express A-CAM. (E) Distinct labelling of fibroblasts and myotubes; formation of the epicardium (arrows point at weakly stained fibroblasts). *cj*, cardiac jelly; *clp*, cardiac lateral plate; *ec*, endocardium; *en*, endoderm; *epc*, epicardium; *mc*, myocardium; *ph*, pharynx. Bar, 50 μ m.

Table 1. Comparative distribution profile of L-CAM and A-CAM in adult chicken non-nervous tissues

Tissues	L-CAM	A-CAM
Skin	+	+
Cornea	+	+
Lens	–	+
Gut	+	–
Kidney	+	–
Liver (hepatocytes)	+	–
Testis (seminiferous tubules)	+	+
Tongue	+	–
Skeletal muscles	–	–
Smooth muscles	–	–
Cardiac muscles	–	+

part of the clefts exhibited a much stronger staining than the ectodermal part, the difference in the staining underlining the boundary between the two tissues (Fig. 12E).

A-CAM distribution in the adult

The distribution of A-CAM was studied in adult non-neuronal tissues and was compared with that of L-CAM. As shown on Table 1, A-CAM was found in the skin, cornea, lens, testis and in cardiac muscles. This pattern of distribution was strikingly restricted as compared to that found in the embryo; tissues that exhibited A-CAM during the whole embryonic life were devoid of A-CAM labelling after hatching; in particular, such is the case of the striated muscles. In contrast to A-CAM, L-CAM was retained on many tissues including the tongue, liver, kidney, gut, cornea and skin. It is noteworthy that the distribution

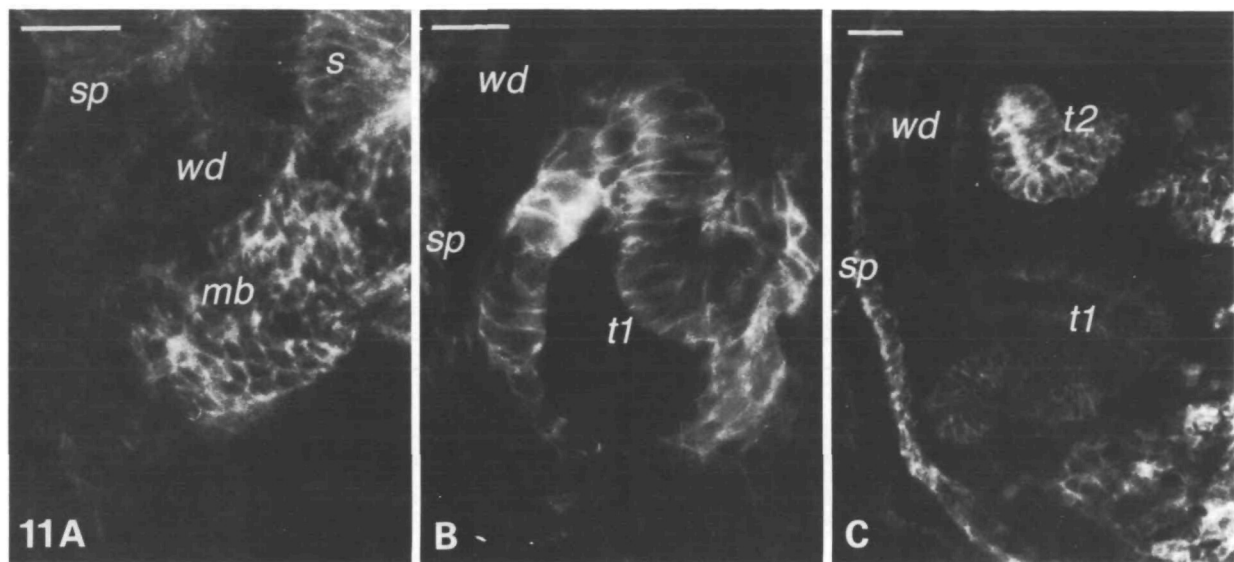


Fig. 11. Distribution of A-CAM during induction of the mesonephric tubules. A, B and C represent three typical stages of the formation of the mesonephric tubules, i.e. the condensation of the mesonephric blastema, the S-shaped tubule and the fully differentiated tubules. A-CAM is present in high amounts on mesonephric cells during the first two steps but at the step shown in C, it progressively disappears from first the primary tubules then from the secondary tubules. *mb*, mesonephric blastema; *s*, somite; *sp*, splanchnic epithelium; *t1*, primary tubules; *t2*, secondary tubules; *wd*, Wolffian duct. (A,C) bar, 50 μ m; (B) bar, 25 μ m.

patterns of L-CAM and A-CAM were largely complementary so that most tissues possess one calcium-dependent mode of cell adhesion.

Embryonic forms of A-CAM

In order to compare the molecular properties of embryonic A-CAM to the one found in adult tissues, we have extracted lens and heart tissues from adult chicks as well as 5-day chick embryos, run the extracts on SDS-polyacrylamide gels and subjected the gels to immunoblotting analysis. As shown in Fig. 13, significant differences were detected in the relative migrations of the embryonic and adult A-CAM, the latter displaying a higher molecular weight. The apparent differences correspond to about 5×10^3 .

Discussion

Recent studies on A-CAM have shed light on its structure, cellular distribution and possible function. In particular, it was shown that the molecule is a membrane component of adherens-type junctions, the major portion of which is extending into the junctional cleft (Volk & Geiger, 1984, 1986a). Furthermore, antibody-inhibition studies indicated that this molecule is involved in a calcium-dependent cell-to-cell attachment (Volk & Geiger, 1986b). In the present study, we have extended these observations and examined the spatiotemporal expression of A-CAM in chicken embryos. We have shown here that

A-CAM is present in cells derived from all three germ layers. In contrast to the adult chicken in which the expression of A-CAM is restricted to a limited number of tissues (i.e. cardiac muscle and eye lens), this protein is transiently present in many embryonic epithelia in which it is apparently involved in morphogenetic and histogenetic processes.

Two coupled features of A-CAM are its apparent capacity to mediate cell-cell adhesion and consequently to initiate the assembly of the actin and vinculin-containing cytoskeletal and plaque domains at the endofacial surface of the membrane (Volk & Geiger, 1986a,b). These two processes are apparently closely interrelated with each other since the establishment of contact seems to be essential for the local induction of microfilament assembly which, in turn, may not only stabilize the intercellular adhesion, but also act as a contractile force-generating system. The two functions of A-CAM are reflected in its spatial distribution during epithelialization of tissues. It is at first present diffusely on the surface of regrouping cells, then it becomes restricted to the subapical surface of cells in association with adherens junctions. We would like, however, to distinguish between these two consequences of A-CAM-mediated interactions since they may play distinct and complementary roles during morphogenesis and tissue shaping.

In the present study, we have described cases in which the expression of A-CAM or its down-regulation is closely correlated with specific epithelialization or with dissociation of epithelial aggregates,

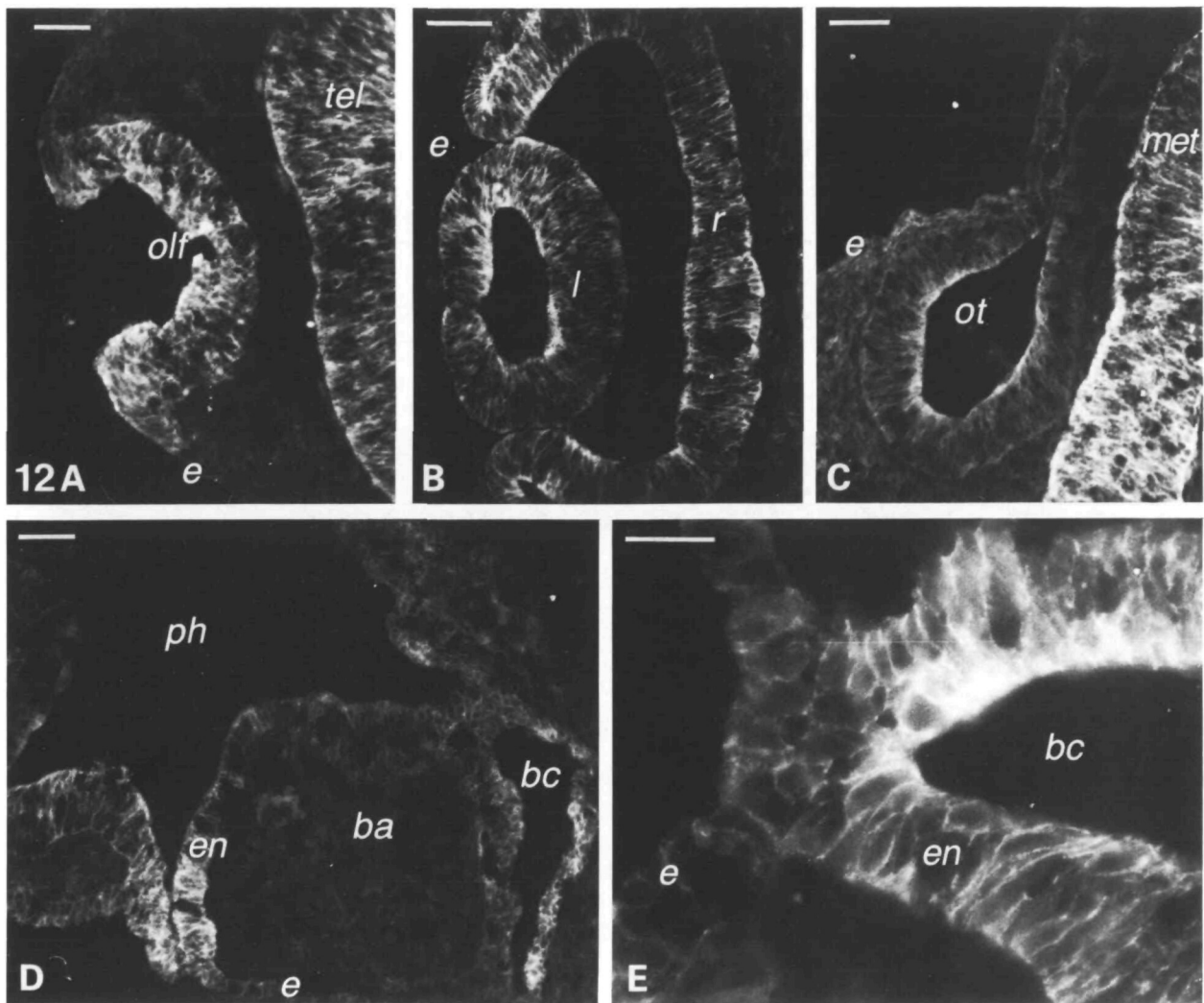


Fig. 12. Distribution of A-CAM in ectodermal placodes and branchial arches. (A) Invaginating olfactory placode heavily stained in contrast to the neighbouring ectoderm which is negative. (B) Lens and retina that both show A-CAM on their surfaces. (C) Fully invaginated otic vesicle. Only the ventral side of the vesicle is stained; notice the weakness of the staining as compared to the neural tube. (D,E) Branchial arches and clefts. The endodermal part of the branchial arch close to the cleft is heavily stained for A-CAM; the ectoderm and the endoderm of the pharynx are also stained but to a lesser extent. E represents a detail of the arch at the junction between the ectoderm and the endoderm. *ba*, branchial arch; *bc*, branchial cleft; *e*, ectoderm; *en*, endoderm; *l*, lens; *olf*, olfactory placode; *ot*, otic vesicle; *met*, metencephalon; *ph*, pharynx; *r*, retina; *tel*, telencephalon. (A–D) bar, 50 μ m; (E) bar, 25 μ m.

respectively. Examples of such relationships for various processes of mesenchymal cell interactions are given in somite formation (see Lash, 1985; Duband *et al.* 1987). Somites are formed by aggregation of mesenchymal cells into elongated rods, namely the segmental plates. During that process, the intensity of labelling with A-CAM antibodies gradually increases and the labelling is apparently concentrated in focal regions along the cell membrane, corresponding to sites of intracellular contact. The next stage in somite formation involves a metameric epithelialization whereby the spherical somites are formed, constructed of polar epithelium with apical epithelialization whereby the spherical somites are formed,

constructed of polar epithelium with apical surface at the luminal sides and surrounded by a peripheral basement membrane. This polarity is also manifested at the level of A-CAM distribution; its apparent content increases and it is found mostly around the subapical region of the cells. Electron microscopic examination of mature somites indicated that, in this region, a conspicuous adherens-type junction is present with actin bundle associated with its endofacial surfaces. Somites are transient structures and, subsequent to their assembly, their medioventral portions, namely the sclerotomes, lose their epithelial organization and dissociate. Labelling for A-CAM indicated that, prior to the apparent dissociation of

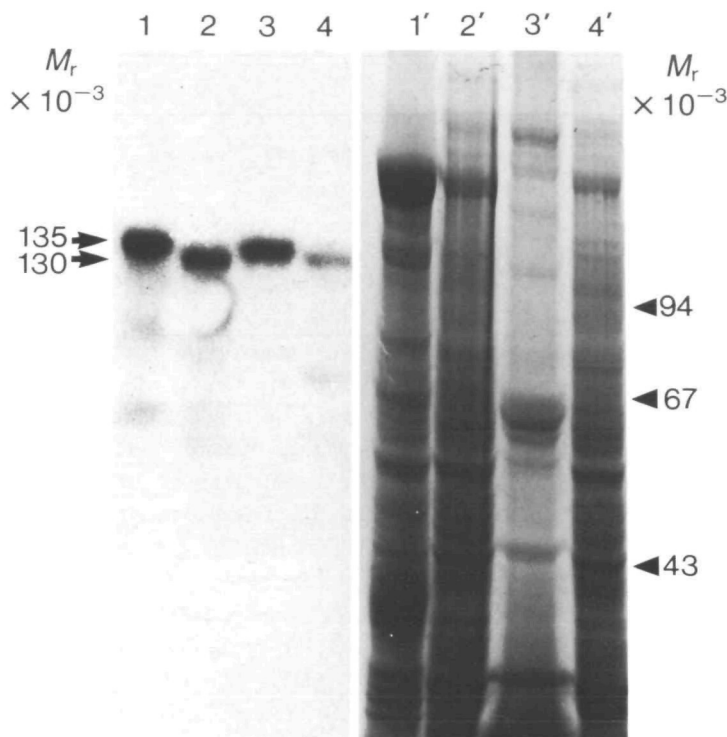


Fig. 13. Immunoblot with antibodies to A-CAM on extracts of heart (lines 1 and 2) and lens (lines 3 and 4) cells from adult chickens and 5-day-old chick embryos, respectively. Lines 1'–4' show the corresponding Coomassie-blue stainings. Both heart and lens cells exhibit an adult and an embryonic form of A-CAM that differ in their apparent molecular weight. The difference corresponds to approximately $3\text{--}5 \times 10^3$, the adult form of A-CAM displaying a higher molecular weight. Note that no difference in molecular weight can be detected between A-CAM found in lens cells and the one of heart cells.

the sclerotome, a drastic reduction of A-CAM levels was noted in the presumptive sclerotomal area. This spatial and temporal coordination between A-CAM level and epithelialization (or de-epithelialization) suggests that A-CAM plays a central role in the regulation of these intracellular interactions. While A-CAM molecules distributed on the whole cell surface may participate in the process of cell aggregation, those present in adherens junctions not only mediate cell–cell adhesion but also induce the assembly of microfilaments. The coordinated modulation of A-CAM during somite formation and dissociation is only a single example illustrating the functional properties of this molecule and a similar set of molecular events was detected in neural crest cells which lost A-CAM at their premigratory stage and regained it during gangliogenesis.

It should, nevertheless, be borne in mind that A-CAM is not the only cell adhesion molecule present in the somites. Previous studies have indicated that

these cells also contain N-CAM and N-cadherin (Thiery *et al.* 1982; Duband *et al.* 1987; Hatta *et al.* 1987). The former is present in the aggregating mesodermal cells, yet is distributed throughout the cell surface, showing no apparent concentration in the area of apical junctions. Furthermore, the levels of N-CAM did not drastically decline prior to dissociation of the sclerotome as did the levels of A-CAM (Duband *et al.* 1987). It should be pointed out that, in contrast to N-CAM, we have found many lines of similarity between A-CAM and N-cadherin. In particular, the two molecules show identical spatiotemporal distributions throughout somitogenesis (Duband *et al.* 1987; Hatta *et al.* 1987), suggesting that they may be related, or even identical.

This similarity between A-CAM and N-cadherin is further substantiated by their almost coincidental distribution patterns during embryogenesis (Hatta & Takeichi, 1986; Hatta *et al.* 1987). Preliminary results show that antibodies to A-CAM (ID 7.2.3.; Volk & Geiger, 1984) and antibodies to N-cadherin (NCD-2; Hatta *et al.* 1987) react with the same molecule in chicken lens cells. In fibroblasts, however, antibodies to A-CAM react with a band displaying a similar molecular weight with which anti-N-cadherin antibodies do not react, suggesting some cell-type-specific variability among these closely related molecules (Volk, T., Takeichi, M. & Geiger, B., unpublished results). The molecular basis, as well as the developmental and functional significance, of this variability are still unclear but it may be reflected in some differences noted between A-CAM localization described here and N-cadherin localization described in Hatta *et al.* (1987). Examples of such differences are the loose mesenchyme along the neural tube in cephalic regions and fibroblasts in the myocardium. Attempts to approach this aspect using side-by-side staining with the two antibodies are now in progress.

A different type of histogenetic reorganization in which A-CAM was apparently involved was characterized by the remodelling of preexisting epithelial sheets as in the case of the ectodermal lens and olfactory placodes and in neurulation. Unlike somite formation in which loosely packed cells were apparently compacted, those processes do not involve aggregation and epithelialization since the ectodermal tissues in which these structures develop already display a polar epithelial morphology prior to A-CAM appearance. Labelling of early embryos with antibodies to other CAMs indicated that prior to neurulation, the entire ectoderm is positively labelled for L-CAM and N-CAM (Thiery *et al.* 1982, 1984; Crossin *et al.* 1985). The spatially restricted expression of A-CAM and, especially, its predominance at the apices of the cells produces some interesting implications concerning the involvement of A-CAM

(and consequently of adherens-type junctions) in the folding of epithelial sheets.

Adherens junctions, such as the ones found in the terminal web of various polarized epithelia, are characterized by their association with bundles of actin filaments (Farquhar & Palade, 1963; Staehelin, 1974). Based on experiments with various tissues and with cultured epithelial cells, it was established that the adherens junction-attached actin cables are under tension leading to a mechanical integration of forces through the entire epithelium (Kartenbeck *et al.* 1982; Geiger *et al.* 1985b; Volk & Geiger, 1986a,b; Volberg *et al.* 1986). Our studies on cultured Madin-Darby bovine kidney and chicken lens cells have shown that dissociation of adherens-type junctions after the removal of extracellular Ca^{2+} was rapidly followed by contraction of the junctional membranes and the associated filament belts (Kartenbeck *et al.* 1982; Volberg *et al.* 1986; Volk & Geiger, 1986b). It thus seems most likely that the presence of A-CAM-containing adherens junctions leads to the assembly of an elaborate contractile apparatus along the subapical aspect of the invaginating neural groove and the various ectodermal placodes. It could further be postulated that the local generation of mechanical forces along the apical regions of these tissues provides the tension necessary for the infolding. This view on the involvement of an apical contractile system in such tissue rearrangements is supported by electron microscopic evidence which points to the presence of junction-bound microfilament bundles in these regions (see, in particular, Begg *et al.* 1978; Geiger *et al.* 1981). One may further propose that the spatially and temporally regulated appearance of A-CAM may provide a primary signal for the local assembly of the microfilament system along the junctional membrane.

Immunofluorescence labelling of A-CAM-containing epithelia at various stages after their formation or reorganization in association with electron microscopic studies revealed an interesting relationship between the distribution of A-CAM and the localization of adherens junctions. As shown in the invaginating neural groove and early neural tube, A-CAM labelling was predominantly concentrated in the subapical regions. Later, this protein was detected also in extrajunctional regions along the lateral cell borders. A likely explanation for this transition may be that the immobilization of A-CAM in the junction may, at some developmental stages, reach saturation and, subsequently, excess of A-CAM will remain in extrajunctional compartments. The function of these extrajunctional A-CAM molecules is not known yet. They may be functionally active and thus participate in the intercellular adhesion or, alternatively, they may constitute a reservoir for the formation of

additional adherens junctions. The nature of the cellular factor(s) which set the limits for further extension of the junction is not clear yet. It might be pointed out that a similar mechanism may also account for some ambiguities concerning the cellular location of L-CAM. This protein was shown by several investigations to be an adherens junction component, yet was also detected in extrajunctional areas (Thiery *et al.* 1984; Boller *et al.* 1985; Volk *et al.* 1987).

It should be mentioned that, beside their similar association with adherens-type junctions, A-CAM and L-CAM appear to differ in their intrinsic capacity to induce the assembly of these junctions; such variations could be responsible for the marked structural differences between the conspicuous junctions present in the neural tube, for example, as compared to those detected throughout the ectoderm. In addition, this functional difference between A-CAM and L-CAM might explain that, during the formation of epithelia such as the kidney and liver, A-CAM is expressed at first at the time of junction formation and, once the epithelium is stabilized, it is replaced by L-CAM. Beside these differences, it should be indicated that A-CAM and L-CAM present some interesting common features. These include the requirement of both molecules for extracellular Ca^{2+} (Gallin *et al.* 1983; Yoshida-Noro *et al.* 1984; Volk & Geiger, 1984) and their capacity to form heterotypic junctions. The latter notion is based on our recent results showing that, when liver cells and lens cells are cocultured, adherens junctions are formed between the two presenting L-CAM on one side and A-CAM on the other (Volk *et al.* 1987). In this respect, it is interesting to note that, in the adult, the distribution patterns of A-CAM and L-CAM are largely complementary so that, in every tissue, adherens junctions contain at least one of these calcium-dependent CAMs.

In conclusion, we propose here that the spatiotemporal modulation of A-CAM during embryogenesis plays a major role in morphogenetic interactions and tissue reorganizations, including cell aggregation, assembly of polar epithelia and invagination of ectodermal placodes.

We would like to thank Talila Volk for helpful discussions. This work was supported by the Muscular Dystrophy Association, the Centre National de la Recherche Scientifique, the Institut National de la Santé et de la Recherche Médicale (CRE 864015), the Fondation pour la Recherche sur la Myopathie and the March of Dimes (1-993). J.L.D. was a recipient of a short-term fellowship from the European Molecular Biology Organization.

References

- BEGG, D. A., RODEWALD, R. & REBHUN, L. I. (1978). The visualization of actin filament polarity in thin sections: Evidence for the uniform polarity of membrane-associated filaments. *J. Cell Biol.* **79**, 846–852.
- BOLLER, K., VESTWEBER, D. & KEMLER, R. (1985). Cell-adhesion molecule uvomorulin is localized in the intermediate junctions of adult intestinal epithelial cells. *J. Cell Biol.* **100**, 327–332.
- CHUONG, C.-M. & EDELMAN, G. M. (1985a). Expression of cell adhesion molecules in embryonic induction. I. Morphogenesis of nestling feathers. *J. Cell Biol.* **101**, 1009–1026.
- CHUONG, C.-M. & EDELMAN, G. M. (1985b). Expression of cell adhesion molecules in embryonic induction. II. Morphogenesis of adult feathers. *J. Cell Biol.* **101**, 1027–1043.
- CROSSIN, K. L., CHUONG, C.-M. & EDELMAN, G. M. (1985). Expression sequences of cell adhesion molecules. *Proc. natn. Acad. Sci. U.S.A.* **82**, 6942–6946.
- DAMSKY, C. H., RICH, J., SOLTER, D., KNUDSEN, K. & BUCK, C. A. (1983). Identification and purification of a cell surface glycoprotein mediating intercellular adhesion in embryonic and adult tissue. *Cell* **34**, 455–466.
- DUBAND, J.-L. & THIERY, J. P. (1985). Adhesive molecules and their role during the ontogeny of the peripheral nervous system. In *Cellular and Molecular Control of Direct Cell Interactions* (ed. H.-J. Marthy). NATO ASI Series, Series A: Life Sciences, pp. 85–118. New York: Plenum Press.
- DUBAND, J.-L., DUFOUR, S., HATTA, K., TAKEICHI, M., EDELMAN, G. M. & THIERY, J. P. (1987). Adhesion molecules during somitogenesis in the avian embryo. *J. Cell Biol.* **104**, 1361–1374.
- EDELMAN, G. M., GALLIN, W. J., DELOUVÉE, A., CUNNINGHAM, B. A. & THIERY, J. P. (1983). Early epochal maps of two different cell adhesion molecules. *Proc. natn. Acad. Sci. U.S.A.* **80**, 4334–4388.
- EDELMAN, G. M. & THIERY, J. P. (1985). *The Cell in Contact: Adhesion and Junctions as Morphogenetic Determinants*, pp. 1–507. New York: John Wiley & Sons.
- EDELMAN, G. M. (1985). Cell adhesion and the molecular processes of morphogenesis. *A. Rev. Biochem.* **54**, 135–169.
- EDELMAN, G. M. (1986). Cell adhesion molecules in the regulation of animal form and tissue pattern. *A. Rev. Cell Biol.* **2**, 81–116.
- FARQUHAR, M. G. & PALADE, G. E. (1963). Junctional complexes in various epithelia. *J. Cell Biol.* **17**, 375–409.
- GALLIN, W. J., EDELMAN, G. M. & CUNNINGHAM, B. A. (1983). Characterization of L-CAM, a major cell adhesion molecule from embryonic liver cells. *Proc. natn. Acad. Sci. U.S.A.* **90**, 1038–1042.
- GEIGER, B., DUTTON, A. H., TOKUYASU, K. T. & SINGER, S. J. (1981). Immunoelectron microscope studies of membrane microfilament interactions: Distributions of alpha-actinin, tropomyosin, and vinculin in intestinal epithelial brush border and chicken gizzard smooth muscle cells. *J. Cell Biol.* **91**, 614–628.
- GEIGER, B., VOLK, T. & VOLBERG, T. (1985a). Molecular heterogeneity of adherens junctions. *J. Cell Biol.* **101**, 1523–1531.
- GEIGER, B., AVNUR, Z., VOLBERG, T. & VOLK, T. (1985b). Molecular domains of adherens junctions. In *The Cell in Contact: Adhesions and Junctions as Morphogenetic Determinants* (ed. G. M. Edelman & J. P. Thiery), pp. 461–489. New York: John Wiley & Sons.
- HAMBURGER, V. & HAMILTON, H. L. (1951). A series of normal stages in the development of the chick embryo. *J. Morph.* **88**, 49–92.
- HATTA, K. & TAKEICHI, M. (1986). Expression of N-cadherin adhesion molecules associated with early morphogenetic events in chick development. *Nature, Lond.* **320**, 447–449.
- HATTA, K., TAKAGI, S., FUJISAWA, H. & TAKEICHI, M. (1987). Spatial and temporal expression pattern of N-cadherin cell adhesion molecules correlated with morphogenetic processes of chicken embryos. *Devl Biol.* **120**, 215–227.
- HYAFIL, F., MORELLO, D., BABINET, C. & JACOB, F. (1980). A cell surface glycoprotein involved in the compaction of embryonal carcinoma cells and cleavage stage embryos. *Cell* **21**, 927–934.
- KARTENBECK, J., SCHMID, E., FRANKE, W. W. & GEIGER, B. (1982). Different modes of internalization of proteins associated with adherens junctions and desmosomes: Experimental separation of lateral contacts induces endocytosis of desmosomal plaque material. *EMBO J.* **1**, 725–732.
- LASH, J. W. (1985). Somitogenesis: Investigations on the mechanism of compaction in the presomitic mass and a possible role of fibronectin. In *Developmental Mechanisms: Normal and Abnormal* (ed. J. W. Lash & L. Saxén), pp. 45–60. New York: Alan R. Liss.
- LOHMANN, S. M., WALTER, U., MILLER, P. E., GREENGARD, P. & DE CAMILLI, P. (1981). Immunohistochemical localization of cyclic GMP-dependent protein kinase in mammalian brain. *Proc. natn. Acad. Sci. U.S.A.* **78**, 653–657.
- MURRAY, B. A., OWENS, G. C., PREDIGER, E. A., CROSSIN, K. L., CUNNINGHAM, B. A. & EDELMAN, G. M. (1986). Cell-surface modulation of the neural cell-adhesion molecule resulting from alternative mRNA splicing in a tissue-specific developmental sequence. *J. Cell Biol.* **103**, 1431–1439.
- NOSE, A. & TAKEICHI, M. (1986). A novel cadherin cell adhesion molecule: Its expression patterns associated with implantation and organogenesis of mouse embryos. *J. Cell Biol.* **103**, 2649–2658.
- ÖBRINK, B. (1986). Epithelial cell adhesion molecules. *Expt Cell Res.* **163**, 1–21.
- OCKLIND, C., FORSUM, U. & ÖBRINK, B. (1983). Cell surface localization and tissue distribution of a hepatocyte cell-cell adhesion glycoprotein (cell-CAM 105). *J. Cell Biol.* **96**, 1168–1171.

- ODIN, P. & OBRINK, B. (1986). Dynamic expression of the cell-adhesion molecule cell-CAM 105 in fetal and regenerating rat liver. *Expl Cell Res.* **164**, 103–114.
- STAEHELIN, L. A. (1974). Structure and function of intercellular junctions. *Int. Rev. Cytol.* **39**, 191–283.
- THIERY, J. P., DUBAND, J.-L., RUTISHAUSER, U. & EDELMAN, G. M. (1982). Cell adhesion molecules in early chicken embryogenesis. *Proc. natn. Acad. Sci. U.S.A.* **79**, 6737–6741.
- THIERY, J. P., DELOUVÉE, A., GALLIN, W., CUNNINGHAM, B. A. & EDELMAN, G. M. (1984). Ontogenetic expression of cell adhesion molecules: L-CAM is found in epithelia derived from the three primary germ layers. *Devl Biol.* **102**, 61–78.
- VAKAET, L. (1970). Cinematographic investigations of gastrulation in the chick blastoderm. *Archs. Biol.* **81**, 387–426.
- VOLBERG, T., GEIGER, B., KARTENBECK, J. & FRANKE, W. (1986). Changes in membrane-microfilament interaction in intercellular adherens junctions upon removal of extracellular calcium ions. *J. Cell Biol.* **102**, 1832–1842.
- VOLK, T. & GEIGER, B. (1984). A 135-kd membrane protein of intracellular adherens junctions. *EMBO J.* **3**, 2249–2260.
- VOLK, T. & GEIGER, B. (1986a). A-CAM: A 135-kD receptor of intercellular adherens junctions. I. Immunoelectron microscopic localization and biochemical studies. *J. Cell Biol.* **103**, 1441–1450.
- VOLK, T. & GEIGER, B. (1986b). A-CAM: A 135-kD receptor of intercellular adherens junctions. II. Antibody-mediated modulation of junction formation. *J. Cell Biol.* **103**, 1451–1464.
- VOLK, T., COHEN, O. & GEIGER, B. (1987). Formation of heterotypic adherens-type junctions between L-CAM-containing liver cells and A-CAM-containing lens cells. *Cell* **50**, 987–994.
- YOSHIDA-NORO, C., SUSUKI, N. & TAKEICHI, M. (1984). Molecular nature of the calcium-dependent cell-cell adhesion system in mouse teratocarcinoma and embryonic cells studied with a monoclonal antibody. *Devl Biol.* **101**, 19–27.

(Accepted 23 February 1988)